



HAL
open science

Fabrication of high aspect ratio microfluidic devices for long term in vitro culture of 3D tumor models

Martina Ugrinic, Dominique Decanini, Nadège Bidan, Gianpiero Lazzari, Abdelmounaim Harouri, Gilgueng Hwang, Anne Marie Haghiri-Gosnet, Simona Mura

► To cite this version:

Martina Ugrinic, Dominique Decanini, Nadège Bidan, Gianpiero Lazzari, Abdelmounaim Harouri, et al.. Fabrication of high aspect ratio microfluidic devices for long term in vitro culture of 3D tumor models. *Microelectronic Engineering*, 2023, 267-268, pp.111898. 10.1016/j.mee.2022.111898 . hal-03832911

HAL Id: hal-03832911

<https://hal.science/hal-03832911>

Submitted on 18 Nov 2022

HAL is a multi-disciplinary open access archive for the deposit and dissemination of scientific research documents, whether they are published or not. The documents may come from teaching and research institutions in France or abroad, or from public or private research centers.

L'archive ouverte pluridisciplinaire **HAL**, est destinée au dépôt et à la diffusion de documents scientifiques de niveau recherche, publiés ou non, émanant des établissements d'enseignement et de recherche français ou étrangers, des laboratoires publics ou privés.

Fabrication of high aspect ratio microfluidic devices for long term *in vitro* culture of 3D tumor models

Martina Ugrinic^{a,b}, Dominique Decanini^b, Nadège Bidan^a, Gianpiero Lazzari^{a,c}, Abdelmounaim Harouri^b, Gilgueng Hwang^b, Anne-Marie Haghiri-Gosnet^{b,*} and Simona Mura^{a,*}.

^a Université Paris-Saclay, CNRS, Institut Galien Paris-Saclay, 92296, Châtenay-Malabry, France

^b Centre de Nanosciences et Nanotechnologies, UMR9001, CNRS, Université Paris-Saclay, 91120 Palaiseau, France

^c Gene Therapy CDMO services, Charles River Laboratoires – Europe Via Indipendenza 11, 23885 Calco (LC) – Italy (*Current affiliation*)

*Corresponding authors.

E-mail addresses: simona.mura@universite-paris-saclay.fr (S. Mura) and anne-marie.haghiri@c2n.upsaclay.fr (A-M. Haghiri-Gosnet)

Abstract:

We developed a simple method to fabricate high aspect ratio 3D microfluidic devices, as geometrically optimized microenvironment for long-term culture of 3D tumor models (i.e., spheroids). The microfluidic device consists of a 2 mm-wide central chamber for spheroid culture flanked by two 976 μm -wide side channels for medium and nutrients supply. To cage hydrogel inside the central chamber, the side channels are isolated using pillar arrays whose geometry has been carefully designed. The role of the height of the central chamber on the growth of heterotypic pancreatic tumor spheroids, made of cancer cells and fibroblasts, was first studied. Predictably, in the 100 μm -high chamber the spheroid cannot grow vertically and exhibits an elongated and horizontally flattened shape. Instead, the tumor spheroid can grow freely in the 300 and 500 μm high chambers and the invasion of individual cells in the surrounding matrix can be observed over a period of 20 days of culture. In a second step, we investigated an original microfluidic design with two distinct heights for the central chamber and the side channels. Such a design, which promotes better resist adherence, could be 3D printed without any resist residue after development. The heterotypic spheroids cultured in this two-level device revealed progressive cell growth and migration, validating this new approach.

Keywords: microfluidics, 3D printing by two-photon polymerization (2PP), 3D culture, tumor models, multicellular tumor spheroids

1. Introduction

The multifaceted role of the tumor microenvironment (TME) in the creation of conditions favorable to cancer cell proliferation, migration, resistance to therapies and thus patient survival is now widely acknowledged [1-4]. The TME, commonly referred to as tumor stroma, consists of an accumulation of supportive cells known as cancer associated fibroblasts (CAFs) [5, 6] and immune cells [7-10] embedded in a dense extracellular matrix (ECM) rich in collagens, fibronectin, proteoglycans and glycoproteins [11]. The latter forms a fibrous block characterized by a high viscoelasticity, small pore size and limited interfibrillar spaces. The intravenous route is the most commonly used for the administration of antitumor therapies. However, the ECM can compromise the successful accumulation of injected drugs in tumor tissues by sequestering them and limiting their diffusion in the extravascular spaces to the target sites [12, 13]. As a result, the effectiveness of treatments may be reduced. In addition to this physical barrier role, the architecture and stiffness of the ECM can mechanically affect the cellular phenotype and further influence disease progression [14-16]. The complex signaling loop between the heterogeneous population of microenvironmental and cancer cells further steer the latter toward a malignant behavior also resulting in low responses to cytotoxic therapies [17-19]. Therefore, a better understanding of the fundamental molecular and cellular features of human disease is necessary to identify new therapeutic targets and thus propose appropriate treatment strategies that will produce the greatest benefit for the patient.

Nevertheless, the development of improved therapeutics requires *in vitro* models capable of reproducing the *in vivo* physio-pathological complexity and having a higher predictive value than conventional 2D cell cultures, which are easy to manipulate, cost effective but too simplistic [20, 21]. The optimal model should reproduce the multiple barrier that characterize the microenvironment of real tumor tissues, mimic the stroma heterogeneity and plasticity observed *in*

vivo in patients and recreate microenvironmental clues (*e.g.*, soluble and mechanical) that dictate the phenotype of stroma and cancer cells.

In an effort to reach this goal, three-dimensional (3D) cell cultures have been proposed as an alternate approach [21-23]. Of them, spherical cell aggregates, known as multicellular tumor spheroids (MCTS), are extensively studied for drug screening in the field of oncology, owing to their ability to reproduce *in vitro* important characteristics of tumors *in vivo* (*e.g.*, proliferative and metabolic gradients, cell to cell and cell to TME cross-talk) [24, 25].

Thus, for example, the combination of MCTS and ECM-mimicking hydrogels scaffolds has first been described [26, 27], but these constructs, while valuable and insightful, do not completely emulate the biology of the tumors and the absence of perfusion prevents the mechanical and chemical cues generated by the flow from being reproduced [28].

In this context, microfluidics-based models, also known as organs-on-a-chip (and/or tumor on a chip) [29], have received widespread interest to better capture *in vitro* how tumors behave *in vivo*, and for evaluations of drugs under more realistic conditions [30-35]. Since microfluidics allows precise manipulation of fluids in microchannels/chambers, these models can recreate the features of the tumor microenvironment, including blood flow and biochemical gradients, with a greater degree of detail. As such, by exploiting microfluidic platforms it has been possible to (*i*) model vascularized organs and pathological conditions [32, 36-38], (*ii*) mimic vascular pathophysiology [37, 39-41], (*iii*) assess tumor-induced angiogenesis, cell invasion, and metastasis [31, 42-44] as well as (*iv*) evaluate the anticancer and/or antiangiogenic performance of drugs and nanomedicines delivered by a controlled flow [45-49].

The micro- and nanoengineering techniques used to manufacture such advanced devices for spheroid culture are mainly based on conventional soft lithography along with optical lithography for the fabrication of the resist master mold. However, since standard UV lithography is limited in

resist thickness to about 100-200 μm [50], its implementation has resulted in the development of fluidic systems with this restricted height. And, for example, microchambers and channels of this size appeared to be well adapted to study formation of vascular networks in chips loaded with cocultures of endothelial cells and fibroblasts or mesenchymal stem cells [39-41]. In the oncology field, the biomimetic character of such models can be increased by introducing into the microfluidic device multicellular tumor spheroids and combining cancer cells and stromal components embedded within a gel matrix.

Nevertheless, a major concern remains. Indeed, to allow the study of tumor development and to evaluate the efficacy of therapies over time, the fluidic device should be tailored to accommodate a growing spheroid, whose size increases progressively. High-aspect ratio devices are a potentially valuable option, but fabrication of systems with these properties is technically challenging.

Though 250 μm -thick molds based on dry films have been proposed to increase the height of the fluidic culture chamber [30], the extensive application of tumor on a chip in the biomedical field would greatly benefit from the development of new versatile and low-cost methods [51-53].

This work has addressed this issue. We applied the 3D lithography for the fabrication of a master mold with high aspect ratio and combined it with soft lithography in epoxy resist. This would permit low-cost, large-scale manufacture of series of fluidic devices.

In order to produce in a single step complex and highly resolute 3D structures, we opted for the Direct Laser Writing (DLW) via two-photon polymerization (2PP) (Fig. 1), a prototyping technique that has attracted enormous research attention because of its high spatial resolution and ultraprecision in photopolymerization at both the micro and nanoscale [54, 55].

We have produced systems with unique height (H) in the in the range 100 - 500 μm as well as original devices combining different heights for the central chamber and the lateral fluidic channels (100 and 500 μm , respectively).

Whereas the pioneering work of Kumi *et al* in 2010 [56] demonstrated the successful use of 2PP lithography in modified SU8 resist for arbitrary cross-sections and high aspect ratio, we herein illustrated the high performances of IP-Q resist for direct immersion writing up to 500 μm .

Once the device was fabricated, 4 days-old heterotypic pancreatic cancer spheroids, used as a model of a tumor with a strong fibrotic reaction (*that is*, an abundant stroma), have been herein loaded and cultured. The described influence of mechanical cues on tumor progression and metastatisation [57-59] prompted us to evaluate whether the available space (*that is*, the device aspect ratio) could have affected the growth of spheroids.

We provided the proof of concept that these devices are suited to the long-term culture of the spheroids, and that their geometry influences the structural integrity of the tumor nodule and the invasiveness of individual cells moving from the spheroid in the surrounding matrix.

2. Materials and methods

2.1 Device design and fabrication of the master molds using 2PP lithography

The microfluidic device is composed of a central 2 mm-wide chamber flanked by two 976 μm -wide side channels. For the conventional chamber height of 100 μm , these adjacent channels are separated by arrays of elongated hexagonal pillars having a length of 300 μm and width of 86.6 μm and placed at a distance of 100 μm (Fig. 2a-c). The presence of the pillars allows the hydrogel matrix to be caged in the central chamber and separated from the lateral channels where cell dispersions are introduced individually.

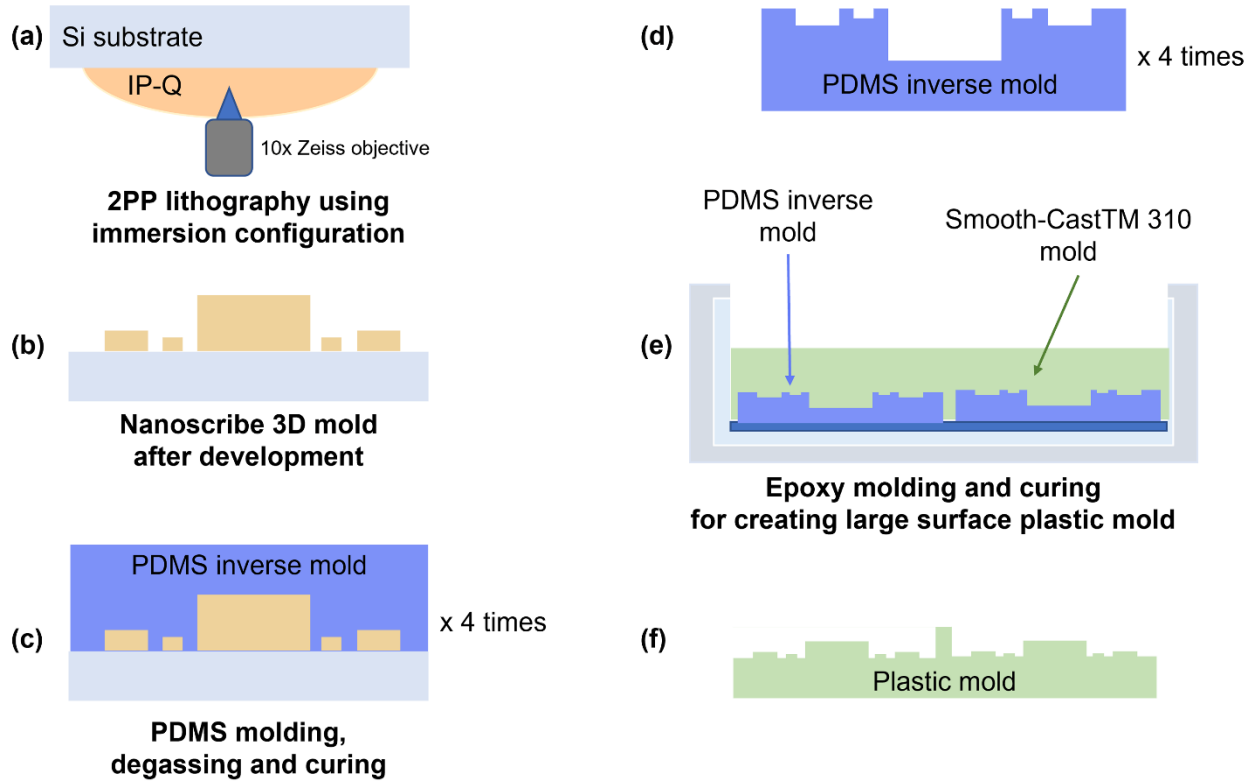


Fig. 1. Schematic diagram of the process flow for (a-b) the fabrication of the IP-Q master mold and its replication, first (c-d) in PDMS several times and finally (e) in epoxy (Smooth-CastTM 310) to get (f) a large surface robust plastic mold.

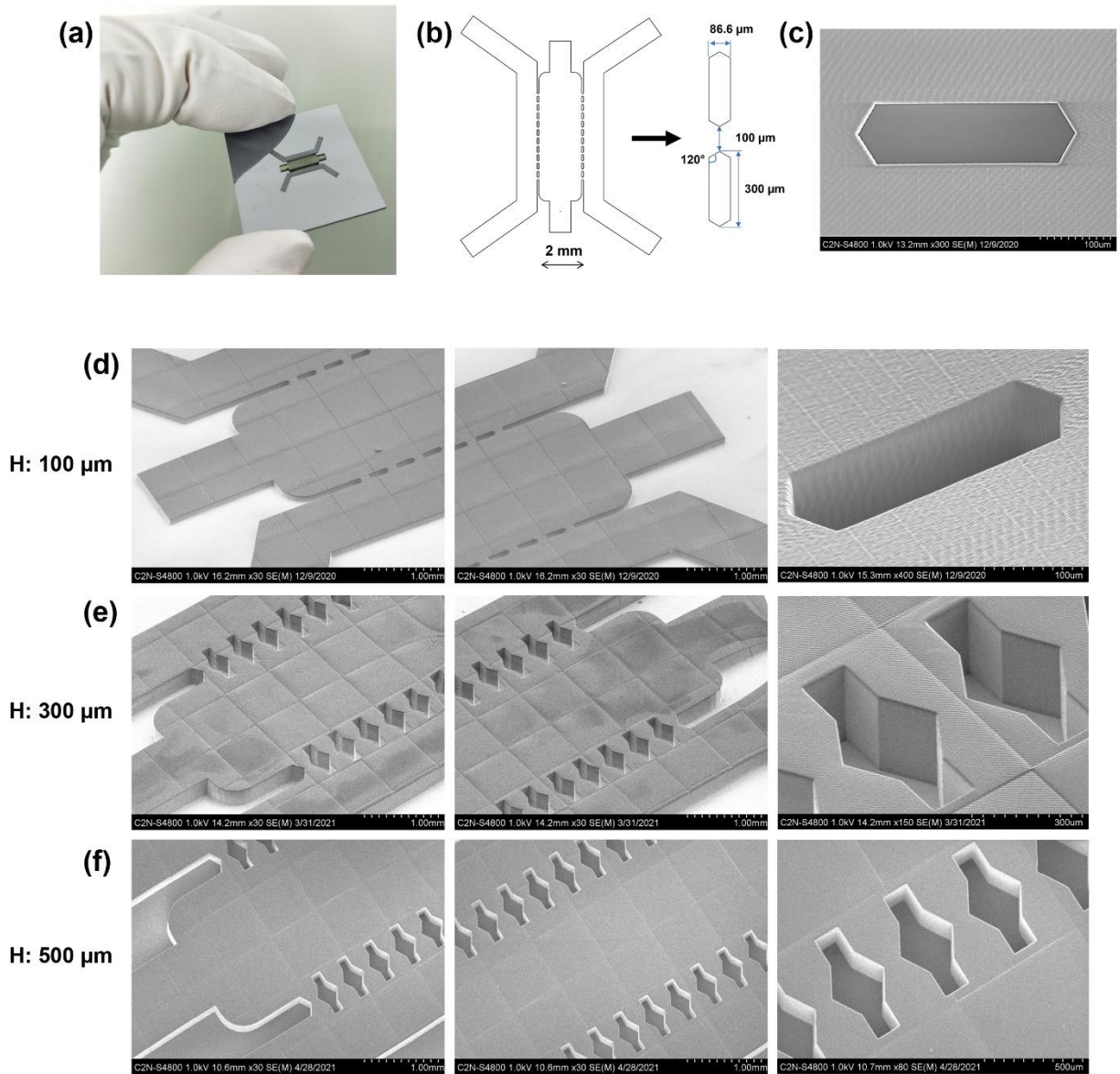


Fig. 2. (a) Optical image of a 3D IP-Q master mold on the 2.5 x 2.5 cm square Si substrate (step (b) of Fig. 1) with (b) a top-view of the design showing the central chamber isolated from the two lateral channels by (b, c) hexagonal structures. (d-f) Side view SEM images of 3D IP-Q molds with thickness ranging from 100 to 500 μm with magnification on the pillar microstructures.

The flow chart presented in Fig. 1 describes all the different technological steps for the fabrication of both the 2PP resist master mold and its copy in a robust plastic on a large surface. First we describe the fabrication of the master mold using 2PP. All microfluidic designs were 3D created using AutoCAD 2021 (Autodesk, Switzerland), and converted to Standard Tessellation Language (STL). Master molds were then printed using a Nanoscribe Photonic Professional GT+ system (Nanoscribe GmbH & Co. KG) with the IP-Q resin. The latter is a photoresist designed for Dip-in Laser Lithography (DiLL) having the properties of high-speed fabrication of mesoscale structures with printing volumes greater than 10 mm³. We opted for this photoresist as it is very stable and full compatible with soft lithography processes such as molding in epoxy. Several designs with different pillar geometry have been investigated to facilitate a perfectly printed mold. Device with a unique channel height (*i.e.*, 100 μm (n=15), 300 μm (n=15) and 500 μm (n=12)) as well as double height devices (*that is*, lateral channels of 100 μm and central chamber of 500 μm, n=29) were prepared and successfully loaded with the spheroids.

While the 2PP process produced a clean structure at 100 μm in height (Fig. 2d), the hexagonal shape of the pillars made the clearing of the resist at 300 and 500 μm in height more difficult. Thus, a second original design with channel height $H = 300$ and 500 μm was proposed (Fig. 2e-f). The shape of the pillar was modified by combining a hexagon (300 μm in width) and a perpendicular rectangular form (total length 600 μm) while keeping the 120° angle. This widening was meant to allow for more accessible flushing of the resist residues from the pillar holes resulting in improved 300 and 500 μm printed molds with clear pillars (Fig. 2e-f, $H=300$ and 500 μm, magnifications). This modification allowed for more efficient casting of the polydimethylsiloxane (PDMS) without its breakage in the pillar region. In addition, this second design with perpendicular rectangular structures should promote a better caging of the hydrogel in the central chamber.

A simple hexagon-shaped pillar (300 μm in width and length) was chosen for the double-height devices (Fig. 6a).

2.2 *Fabrication of the large surface epoxy molds*

Since exposure time using 2PP process can reach several hours and also to preserve the IP-Q master mold, it is of great importance to provide a simple replication process to easily copy each IP-Q 3D master mold in a robust plastic master. Although several epoxies have been extensively studied, Smooth-CastTM 310 was chosen based on its already fully demonstrated simplicity [60], as an interesting way to replicate silicon masters.

We propose here a very simple replication process based on classical molding, degassing and curing as depicted in Figure 1 (Fig. 1c-f). A primary inverse PDMS replica was obtained on each master mold by casting Sylgard 184 silicon elastomer (Dow Corning, USA) (Fig. 1c). Briefly, the PDMS was prepared and mixed in a 10:1 ratio of base (dimethylsiloxane, dimethylvinyl-terminated, and trimethylated silica) to curing agent (Tetrakis (trimethylsilyloxy) silane), degassed under vacuum, and then poured onto a master mold to a height of 2 mm. The PDMS was then left to cure in an oven at 60 °C overnight. Afterwards, the cured PDMS structure was peeled off the master. This process was repeated to build several PDMS inverse replica from the same master mold. In a second step, several replicated PDMS molds were fixed with double-sided adhesive tape (Tesa, Germany), with channels facing upward, on the bottom of a Petri dish, previously coated with Scotch adhesive tape (3M, USA) (Fig. 1e). In order to remove any air trapped in the PDMS, the petri dish was placed in the vacuum chamber for 2 hours. Smooth-CastTM 310 (Smooth-On Inc., USA) plastic resin was mixed in A:B parts ratio of 100:90 w/w, poured onto the degassed PDMS mold then covered and left on the bench overnight. Next, the plastic mold was peeled off and placed in the oven at 60 °C for 15 min. The choice of this resin allowed the construction of a

mechanically durable mold for low-cost manufacturing of microfluidics with the possible multiple replications of the PDMS mold.

A typical 4-inch plastic mold obtained from 4 PDMS replicas is shown in Fig. 3a. It should be noted that there is no limitation on the number of replica and, therefore on the size of the plastic mold, given that the horizontal dimensions can be scaled up by expanding the design to 5-, 6- or even 8-inch wafers that are suitable for standard microfabrication technologies. All the microstructures have been replicated with no loss in quality (vertical and pattern definition) as it can be seen in the enlarged images (Fig. 3b-c).

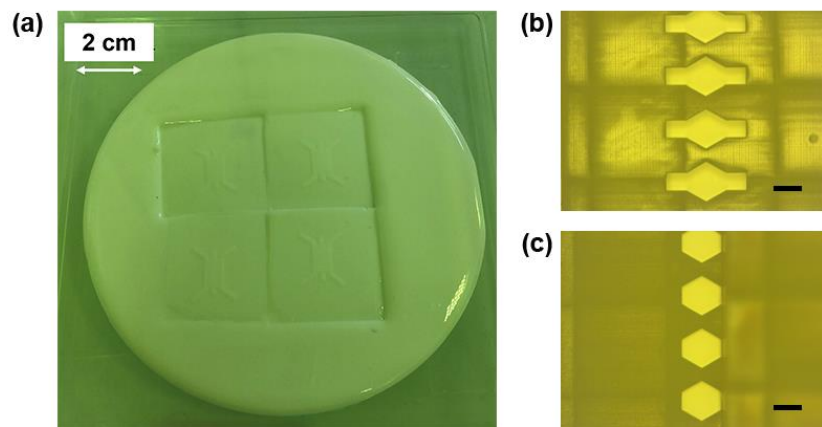


Fig. 3. Replication process in epoxy resist. (a) image of the obtained large surface replicated mold for the production of 4 chips; (b, c) magnification on the pillars proving the quality of replication (scale bars: 200 μm).

2.3 Fabrication of the PDMS devices

Microfluidic devices were fabricated according to the standard PDMS soft-lithography process previously described. The PDMS was prepared, mixed in a 10:1 ratio of base to curing agent, degassed under vacuum, and then poured onto a large surface plastic mold, and left to cure in an

oven at 60 °C for at least 2 hours. After peeling-off the cured PDMS from the plastic mold, inlet and outlet ports as well as a central well were created using a 2- and 1-mm punch (Reusable Rapid Punch Biopsy Kit, World Precision Instruments, France), respectively. Then, the surfaces of the channel side and of a 22 x 22 mm cover glass (Rogo-Sampaic, France) were activated (90 seconds) with an air plasma cleaner (Harrick plasma, USA), placed in contact and sealed. Immediately after, the assembly was placed in an oven at 80 °C for at least 8 hours to ensure complete bonding.

2.4. Cell lines

The PANC-1 cell line (CRL-1469TM) was acquired from ATCC and cultured in Dulbecco's Modified Eagle Medium (DMEM, Sigma Aldrich, France) containing 10% heat-inactivated fetal bovine serum (FBS, Gibco, France). The CAF08 cell line was bought from Vitro Biopharma (USA) and cultured in Pancreatic Stellate CAF Maintenance medium (PC00B5, Vitro Biopharma, USA). The two media were complemented with penicillin (50 U.mL⁻¹) and streptomycin (0.05 mg.mL⁻¹). Cells were incubated at 37°C in 5% CO₂ and used under passage 8 for all experiments.

2.5. Construction of heterotypic spheroids

Heterotypic spheroids made of PANC-1 and CAF08 were formed by cell assembly in nonadherent plates (*that is*, the liquid overlay technique) as earlier reported [61-62]. In brief, cellular suspensions of PANC-1 and CAF08 cells were freshly prepared in DMEM complete medium complemented with 25 ng.mL⁻¹ of hFGF (Human Fibroblastic Growth Factor, F0291, Sigma). Next, 200 µL of their opportune mix was added to the wells of 96 round-bottom well plates (CELLSTAR®, Sigma) previously coated with 50 µL of 1.2% (w/v) poly-2-hydroxyethyl methacrylate (poly-HEMA, Sigma) ethanolic solution. After a centrifugation step (200 g, 5 min,

room temperature), the cells were promptly incubated at 37°C with 5% CO₂ to permit the creation of the spheroids. The number of PANC-1 was set at 1000 cells per well. A PANC-1:CAF08 ratio of 1:4 was used [62].

2.6 Cell seeding in the microfluidic device

After 4/5 days of culture, individual spheroids were harvested and then embedded in a fibrin-collagen gel matrix as previously described, with minor modifications [40]. First, fibrinogen (F8630, Sigma Aldrich, France) was dissolved in phosphate-buffered saline (PBS) at a concentration of 2.8 mg.mL⁻¹. Next 107.2 µL of this solution was combined with 8.0 µL of neutralized rat tail collagen I (3 mg.mL⁻¹, A10483-01, Gibco, France), and 4 µL of aprotinin (4 U.mL⁻¹, A1153, Sigma Aldrich, France). Keeping the tube on ice to avoid gelation, for each spheroid, 99 µL of the resulting solution (*i.e.*, fibrinogen, collagen and aprotinin) was transferred to an Eppendorf tube and combined with 1 µL of thrombin (50 U.mL⁻¹, T4648, Sigma Aldrich, France). Meanwhile, the spheroid was collected from the 96-well plate and transferred, along with the minimum amount of medium, into another tube containing 7 µL of the final mixture (*i.e.*, fibrinogen, collagen, aprotinin and thrombin).

The resultant embedded spheroid was then loaded into the central chamber of the device and successively incubated for 15-30 minutes at 37°C to allow gelation to occur. Afterwards, medium (40 µL) was filled into the side channels. The device was then placed in a petri dish with a humidified Kimwipe to avoid evaporation of the medium and kept in the incubator at 37 °C and 5% CO₂. Half of the medium was renewed every other day, until day 8 (n=2-3) or day 20 (n=1). Spheroids were monitored at regular intervals using an optical microscope equipped with a 10x objective.

3. Results and discussion

Once embedded in the gel matrix, individual spheroids were introduced in the central chamber of the device and cultured for up to 20 days with regular medium replacement (Fig. 4). The appropriately shaped pillars ensured retention of the fibrinogen/collagen hydrogel without leakage in the side channels and the formation of a well-defined medium/hydrogel interface (Fig. 4b).

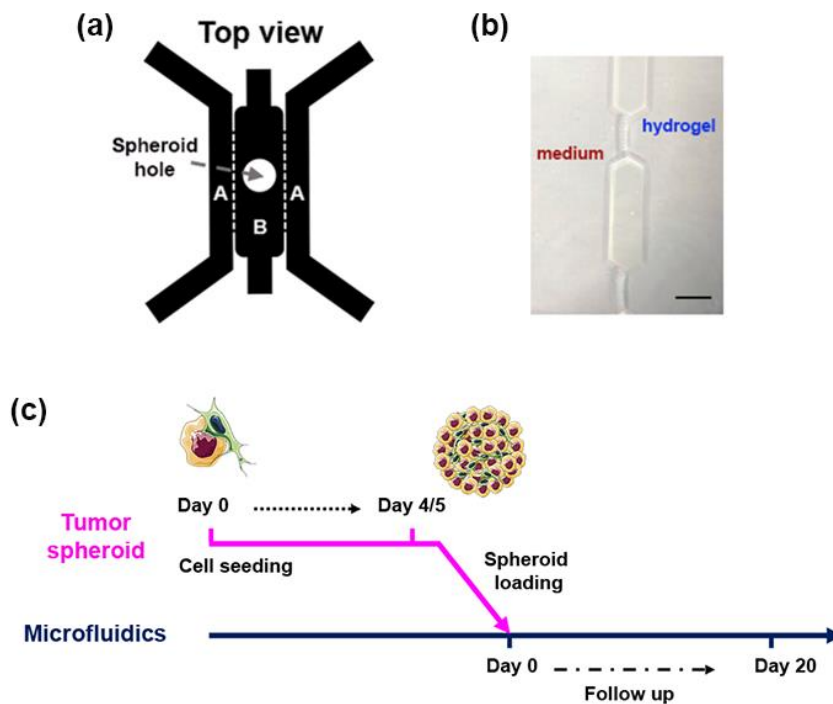


Fig. 4. (a) Design of the microfluidic device showing the fluidic channels (A) flanking the central chamber (B) in which a hole (1 mm large) for spheroid loading has been punched; (b) close up on the medium/hydrogel interface, scale bar: 100 μm ; (c) schematic of the experimental setup.

In the lowest channels (Fig. 5, 100 μm), likely due to the restricted space available, the spheroid appeared to be flattened and grew mainly horizontally in an almost oblong fashion. In contrast, the

increased volume available in the 300 and 500 μm high devices allowed the spheroid to form a spherical mass from which isolated cells came out and the migrated into the central chamber. The migratory front appeared to be directed preferentially towards the inlet of the medium, probably due to the formation of a nutrient gradient in the device during time. At a certain distance from the primary spheroid, the aggregation of cells forming a secondary nodule could also be detected after 14 days for both $H=300$ and $500 \mu\text{m}$ (Fig. 5, day 14 and 20).

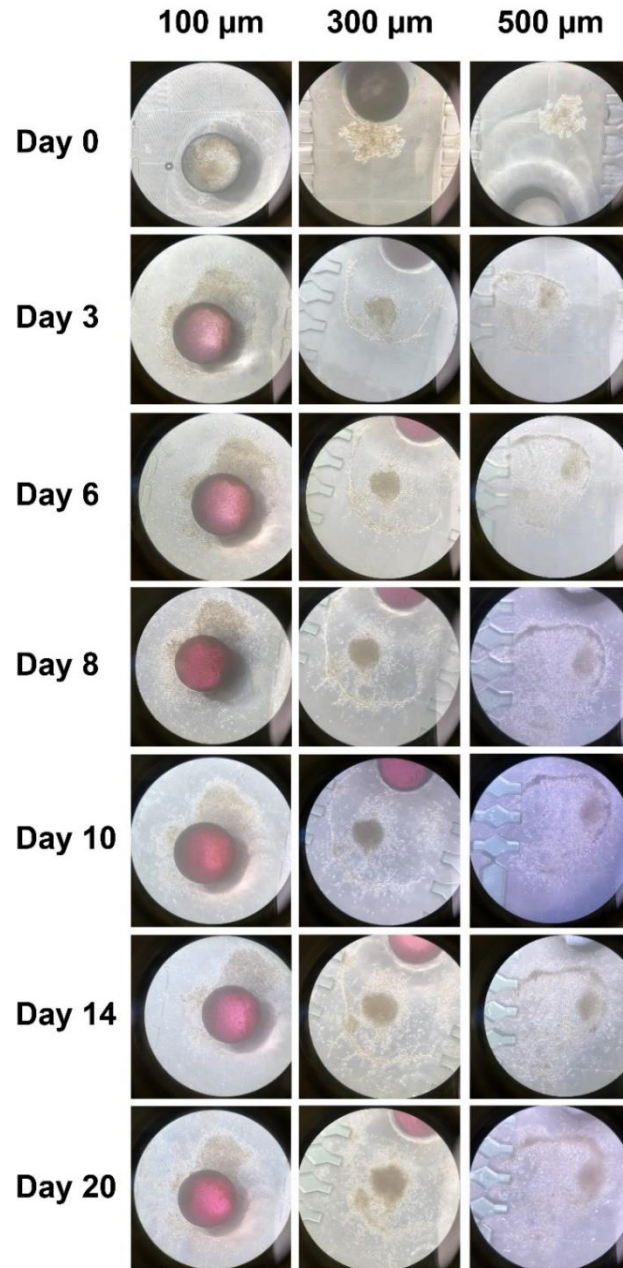


Fig. 5. Representative optical images of PANC-1:CAF08 spheroids growth in the 100, 300 and 500 μm high devices over a period of 20 days. The spheroids were cultured for 4/5 days before being introduced *via* the punched hole (1 mm diameter; black border inner ring in the images) into the microfluidic device: day 0 refers to the day of transfer.

In spite of allowing cell growth and proliferation, thick adjacent channels can favor air bubbles generation during medium refilling. Thus, we further improved the device design by developing a two-height chip with a 500 μm -high central chamber flanked by two 100 μm -high perfusable side channels (Fig. 6a). Thanks to the 2PP lithography using the Nanoscribe system, the patterning of this more advanced 3D system did not present any difficulty. With this two-height design, the master mold could be printed without leftover residue in the hexagon-shaped pillar holes and with a better adherence of the resist to the substrate.

Follow-up of the heterotypic spheroids in the device revealed a progressive cell growth and migration, albeit at a slower rate than in the single-height device, presumably as a result of a dissimilar gradient pattern.

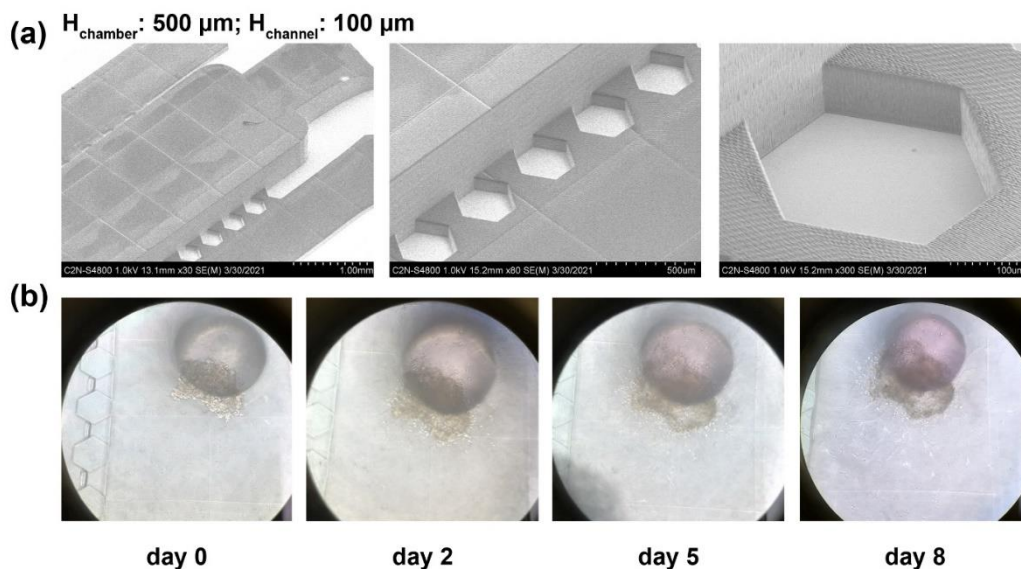


Fig. 6. (a) Side view SEM images of two-layered microfluidic IP-Q 3D master mold with the 500 μm -thick central chamber and the 100 μm -thick lateral channels, and magnification on the pillar structure; (b) representative images of PANC1:CAF08 heterotypic spheroids cultured in the device over a period of 8 days. Day 0 indicates the day of spheroid transfer *via* the punched hole (1 mm diameter; black border inner ring in the images).

4. Conclusion

Various tumor-on-a-chip models have been developed so far but the architecture, composition and dialogue between cells still need to be more closely reproduced to obtain valuable answers to questions related to the spatio-temporal evolution of the tumor-microenvironment pair.

We have proposed a fabrication process to produce 3D fluidic devices with adapted aspect ratio for long term culture of tumor spheroids. 2PP lithography using the Nanoscribe system was applied for the fabrication of a master mold with different heights, for the fluidic adjacent channels and for the spheroid chamber, up to 500 μm . To ensure large-scale manufacture of series of fluidic devices at low cost, a very simple replication process in epoxy resist was also proposed to produce mold replica on large surface. Then, heterotypic pancreatic cancer tumor spheroids, used as a model of a tumor with a strong fibrotic reaction, have been loaded and cultured in the device. If the height of the central chamber is too small and limited to 100 μm , the spheroid appears flattened and can only grow horizontally due to the restricted space available. Raising the height of the chamber to 500 μm promotes more gradual cell growth and migration, thanks to the availability of space for spheroid evolution. Thus, by adjusting the aspect ratio, we have designed and investigated different devices. And, we have provided a proof of concept of the opportunity for their application for tumor spheroids culture.

They might find potential application as a tool to gain in-depth knowledge of how the microenvironment (*e.g.*, biochemical and biomechanical cues) governs tumor function (*e.g.*, growth and migratory capacity) but also how cells affect their 3D environment (*e.g.*, matrix degradation, creation of metabolic gradients).

A detailed characterization of the spatio-temporal evolution of tumor spheroids is in progress. In a second step, the tumor physiopathology will be reproduced by culturing endothelial cells in the external channel until confluence. To ensure optimal cell attachment, the surface of the device

will be suitably treated, for instance by coating it with a mixture of albumin and heparin, as described previously [63]. Then, their barrier function can be modulated by exposing the cells to different cytokines to mimic the increased permeability and retention (EPR) effect observed in a variety of tumors. The introduction of an immune component (*e.g.*, tumor-associated macrophages, Treg cells) whose key role in tumor progression and metastatic spread is widely recognized, will further enhance the biomimetic character of the device.

The use of cell lines was chosen to facilitate the validation of the device, while overcoming constraints related to the availability of biological material, but the use of patient-derived cells is a foreseen attractive option to increase the preclinical value of the device and to study *in vitro* but "*like in humans*" the tumor, its evolution and thus identify the best strategies for a better management of the disease.

Acknowledgments

This work has been supported by a public grant overseen by the French National Research Agency (ANR) as part of the “Investissements d’Avenir” program (reference: ANR-10-LABX-0035, Labex NanoSaclay)” and by the Fondation ARC pour la recherche sur le cancer (PJA20181207698). Miss Stephanie Denis (Institut Galien Paris-Saclay) is kindly acknowledged for her support to the cell culture activities. CNRS and the French Ministry of Research are also warmly acknowledged for financial support.

Data availability statement

The data that support the findings of this study are available from the corresponding author upon request.

References

- [1] R. Baghban, L. Roshangar, R. Jahanban-Esfahlan, K. Seidi, A. Ebrahimi-Kalan, M. Jaymand, S. Kolahian, T. Javaheri, P. Zare, Tumor microenvironment complexity and therapeutic implications at a glance, *Cell Commun. Signal.* 18 (2020) 59, <https://doi.org/10.1186/s12964-020-0530-4>
- [2] D.C. Hinshaw, L.A. Shevde, The Tumor Microenvironment Innately Modulates Cancer Progression, *Cancer Res.* 79 (2019) 4557-4566, <https://doi.org/10.1158/0008-5472.CAN-18-3962>
- [3] E. Karamitopoulou, Tumour microenvironment of pancreatic cancer: immune landscape is dictated by molecular and histopathological features, *Br. J. Cancer* 121 (2019) 5-14, <https://doi.org/10.1038/s41416-019-0479-5>
- [4] B. Lim, W.A. Woodward, X. Wang, J.M. Reuben, N.T. Ueno, Inflammatory breast cancer biology: the tumour microenvironment is key, *Nat. Rev. Cancer* 18 (2018) 485-499, <https://doi.org/10.1038/s41568-018-0010-y>
- [5] E. Sahai, I. Astsaturov, E. Cukierman, D.G. DeNardo, M. Egeblad, R.M. Evans, D. Fearon, F.R. Greten, S.R. Hingorani, T. Hunter, R.O. Hynes, R.K. Jain, T. Janowitz, C. Jorgensen, A.C. Kimmelman, M.G. Kolonin, R.G. Maki, R.S. Powers, E. Puré, D.C. Ramirez, R. Scherz-Shouval, M.H. Sherman, S. Stewart, T.D. Tlsty, D.A. Tuveson, F.M. Watt, V. Weaver, A.T. Weeraratna, Z. Werb, A framework for advancing our understanding of cancer-associated fibroblasts, *Nat. Rev. Cancer* 20 (2020) 174-186, <https://doi.org/10.1038/s41568-019-0238-1>
- [6] Z. Liao, Z.W. Tan, P. Zhu, N.S. Tan, Cancer-associated fibroblasts in tumor microenvironment – Accomplices in tumor malignancy, *Cell. Immunol.* 343 (2019) 103729, <https://doi.org/10.1016/j.cellimm.2017.12.003>
- [7] X. Lei, Y. Lei, J.-K. Li, W.-X. Du, R.-G. Li, J. Yang, J. Li, F. Li, H.-B. Tan, Immune cells within the tumor microenvironment: Biological functions and roles in cancer immunotherapy, *Cancer Letters* 470 (2020) 126-133, <https://doi.org/10.1016/j.canlet.2019.11.009>
- [8] X. Xiang, J. Wang, D. Lu, X. Xu, Targeting tumor-associated macrophages to synergize tumor immunotherapy, *Signal Transduct. Target. Ther.* 6 (2021) 75, <https://doi.org/10.1038/s41392-021-00484-9>
- [9] Y. Pan, Y. Yu, X. Wang, T. Zhang, Tumor-Associated Macrophages in Tumor Immunity, *Front. Immunol.* 11 (2020), <https://doi.org/10.3389/fimmu.2020.583084>

- [10] Q. Yang, N. Guo, Y. Zhou, J. Chen, Q. Wei, M. Han, The role of tumor-associated macrophages (TAMs) in tumor progression and relevant advance in targeted therapy, *Acta Pharm. Sin. B.* 10 (2020) 2156-2170, <https://doi.org/10.1016/j.apsb.2020.04.004>
- [11] C. Frantz, K.M. Stewart, V.M. Weaver, The extracellular matrix at a glance, *J. Cell Sci.* 123 (2010) 4195-4200, <https://doi.org/10.1242/jcs.023820>
- [12] M.W. Dewhirst, T.W. Secomb, Transport of drugs from blood vessels to tumour tissue, *Nat. Rev. Cancer* 17 (2017) 738-750, <https://doi.org/10.1038/nrc.2017.93>
- [13] T. Stylianopoulos, L.L. Munn, R.K. Jain, Reengineering the Physical Microenvironment of Tumors to Improve Drug Delivery and Efficacy: From Mathematical Modeling to Bench to Bedside, *Trends Cancer* 4 (2018) 292-319, <https://doi.org/10.1016/j.trecan.2018.02.005>
- [14] J. Winkler, A. Abisoye-Ogunniyan, K.J. Metcalf, Z. Werb, Concepts of extracellular matrix remodelling in tumour progression and metastasis, *Nat. Commun.* 11 (2020) 5120, <https://doi.org/10.1038/s41467-020-18794-x>
- [15] C.J. Whatcott, C.H. Diep, P. Jiang, A. Watanabe, J. LoBello, C. Sima, G. Hostetter, H.M. Shepard, D.D. Von Hoff, H. Han, Desmoplasia in Primary Tumors and Metastatic Lesions of Pancreatic Cancer, *Clin. Cancer Res.* 1 (2015) 3561-8, <https://doi.org/10.1158/1078-0432.ccr-14-1051>
- [16] E. Henke, R. Nandigama, S. Ergün, Extracellular Matrix in the Tumor Microenvironment and Its Impact on Cancer Therapy, *Front. Mol. Biosci* 6 (2020), <https://doi.org/10.3389/fmolb.2019.00160>
- [17] Y. Ni, X. Zhou, J. Yang, H. Shi, H. Li, X. Zhao, X. Ma, The Role of Tumor-Stroma Interactions in Drug Resistance Within Tumor Microenvironment, *Front. Cell Dev. Biol.* 9 (2021), <https://doi.org/10.3389/fcell.2021.637675>
- [18] B. Son, S. Lee, H. Youn, E. Kim, W. Kim, B. Youn, The role of tumor microenvironment in therapeutic resistance, *Oncotarget* 8 (2017) 3933-3945, <https://doi.org/10.18632/oncotarget.13907>
- [19] P. Wu, W. Gao, M. Su, E.C. Nice, W. Zhang, J. Lin, N. Xie, Adaptive Mechanisms of Tumor Therapy Resistance Driven by Tumor Microenvironment, *Front. Cell Dev. Biol.* 9 (2021), <https://doi.org/10.3389/fcell.2021.641469>
- [20] M.C. Cox, L.M. Reese, L.R. Bickford, S.S. Verbridge, Toward the Broad Adoption of 3D Tumor Models in the Cancer Drug Pipeline, *ACS Biomater. Sci. Eng.* 1 (2015) 877-894, <https://doi.org/10.1021/acsbiomaterials.5b00172>

- [21] K.A. Fitzgerald, M. Malhotra, C.M. Curtin, F.J. O'Brien, C.M. O'Driscoll, Life in 3D is never flat: 3D models to optimise drug delivery, *J. Control. Release* 215 (2015) 39-54, <https://doi.org/10.1016/j.jconrel.2015.07.020>
- [22] C. Jensen, Y. Teng, Is It Time to Start Transitioning From 2D to 3D Cell Culture?, *Frontiers in Molecular Biosciences* 7 (2020), <https://doi.org/10.3389/fmolb.2020.00033>
- [23] M.A. Heinrich, A. Mostafa, J.P. Morton, L. Hawinkels, J. Prakash, Translating complexity and heterogeneity of pancreatic tumor: 3D *in vitro* to *in vivo* models, *Advanced drug delivery reviews* 174 (2021) 265-293, <https://doi.org/10.1016/j.addr.2021.04.018>
- [24] G. Lazzari, P. Couvreur, S. Mura, Multicellular tumor spheroids: a relevant 3D model for the *in vitro* preclinical investigation of polymer nanomedicines, *Polymer Chemistry* 8 (2017) 4947-4969, <https://doi.org/10.1039/C7PY00559H>
- [25] G. Mehta, A.Y. Hsiao, M. Ingram, G.D. Luker, S. Takayama, Opportunities and challenges for use of tumor spheroids as models to test drug delivery and efficacy, *J. Control. Release* 164 (2012) 192-204, <https://doi.org/10.1016/j.jconrel.2012.04.045>
- [26] K.M. Charoen, B. Fallica, Y.L. Colson, M.H. Zaman, M.W. Grinstaff, Embedded multicellular spheroids as a biomimetic 3D cancer model for evaluating drug and drug-device combinations, *Biomaterials* 35 (2014) 2264-2271, <https://doi.org/10.1016/j.biomaterials.2013.11.038>
- [27] D. Yip, C.H. Cho, A multicellular 3D heterospheroid model of liver tumor and stromal cells in collagen gel for anti-cancer drug testing, *Biochem. Biophys. Res. Commun.* 433 (2013) 327-332, <https://doi.org/10.1016/j.bbrc.2013.03.008>
- [28] A. Sontheimer-Phelps, B.A. Hassell, D.E. Ingber, Modelling cancer in microfluidic human organs-on-chips, *Nat. Rev. Cancer* 19 (2019) 65-81, <https://doi.org/10.1038/s41568-018-0104-6>
- [29] S.N. Bhatia, D.E. Ingber, Microfluidic organs-on-chips, *Nat. Biotechnol.* 32 (2014) 760-72, <https://doi.org/10.1038/nbt.2989>
- [30] K.E. Sung, D.J. Beebe, Microfluidic 3D models of cancer, *Adv. Drug Deliv. Rev.* 79-80 (2014) 68-78, <https://doi.org/10.1016/j.addr.2014.07.002>
- [31] M. Chung, J. Ahn, K. Son, S. Kim, N.L. Jeon, Biomimetic Model of Tumor Microenvironment on Microfluidic Platform, *Adv. Healthc. Mater.* 6 (2017), <https://doi.org/10.1002/adhm.201700196>
- [32] B. Zhang, A. Korolj, B.F.L. Lai, M. Radisic, Advances in organ-on-a-chip engineering, *Nat. Rev. Mater.* 3 (2018) 257-278, <https://doi.org/10.1038/s41578-018-0034-7>

- [33] M. Shang, R.H. Soon, C.T. Lim, B.L. Khoo, J. Han, Microfluidic modelling of the tumor microenvironment for anti-cancer drug development, *Lab Chip* 19 (2019) 369-386, <https://doi.org/10.1039/c8lc00970h>
- [34] L. Wan, C.A. Neumann, P.R. LeDuc, Tumor-on-a-chip for integrating a 3D tumor microenvironment: chemical and mechanical factors, *Lab Chip* 20 (2020) 873-888, <https://doi.org/10.1039/c9lc00550a>
- [35] J. Rodrigues, M.A. Heinrich, L.M. Teixeira, J. Prakash, 3D *In vitro* Model (R)evolution: Unveiling Tumor-Stroma Interactions, *Trends Cancer* 7 (2021) 249-264, <https://doi.org/10.1016/j.trecan.2020.10.009>
- [36] L.-D. Ma, Y.-T. Wang, J.-R. Wang, J.-L. Wu, X.-S. Meng, P. Hu, X. Mu, Q.-L. Liang, G.-A. Luo, Design and fabrication of a liver-on-a-chip platform for convenient, highly efficient, and safe in situ perfusion culture of 3D hepatic spheroids, *Lab Chip* 18 (2018) 2547-2562, <https://doi.org/10.1039/C8LC00333E>
- [37] K. Sato, K. Sato, Recent Progress in the Development of Microfluidic Vascular Models, *Anal. Sci* 34 (2018) 755-764, <https://doi.org/10.2116/analsci.17R006>
- [38] K.L. Hayward, S. Kouthouridis, B. Zhang, Organ-on-a-Chip Systems for Modeling Pathological Tissue Morphogenesis Associated with Fibrosis and Cancer, *ACS Biomater. Sci. Eng.* 7 (2021) 2900-2925, <https://doi.org/10.1021/acsbiomaterials.0c01089>
- [39] Y. Nashimoto, T. Hayashi, I. Kunita, A. Nakamasu, Y.S. Torisawa, M. Nakayama, H. Takigawa-Imamura, H. Kotera, K. Nishiyama, T. Miura, R. Yokokawa, Integrating perfusable vascular networks with a three-dimensional tissue in a microfluidic device, *Integr. Biol.* 9 (2017) 506-518, <https://doi.org/10.1039/c7ib00024c>
- [40] Y. Nashimoto, Y. Teraoka, R. Banan Sadeghian, A. Nakamasu, Y. Arima, S. Hanada, H. Kotera, K. Nishiyama, T. Miura, R. Yokokawa, Perfusable Vascular Network with a Tissue Model in a Microfluidic Device, *Journal of visualized experiments : JoVE* (2018), <https://doi.org/10.3791/57242>
- [41] H. Uwamori, T. Higuchi, K. Arai, R. Sudo, Integration of neurogenesis and angiogenesis models for constructing a neurovascular tissue, *Sci. Rep.* 7 (2017) 17349, <https://doi.org/10.1038/s41598-017-17411-0>

- [42] J.S. Jeon, S. Bersini, M. Gilardi, G. Dubini, J.L. Charest, M. Moretti, R.D. Kamm, Human 3D vascularized organotypic microfluidic assays to study breast cancer cell extravasation, *Proc. Natl. Acad. Sci. U S A* 112 (2015) 214, <https://doi.org/10.1073/pnas.1417115112>
- [43] S. Oh, H. Ryu, D. Tahk, J. Ko, Y. Chung, H.K. Lee, T.R. Lee, N.L. Jeon, "Open-top" microfluidic device for *in vitro* three-dimensional capillary beds, *Lab Chip* 17 (2017) 3405-3414, <https://doi.org/10.1039/c7lc00646b>
- [44] Z. Du, S. Mi, X. Yi, Y. Xu, W. Sun, Microfluidic system for modelling 3D tumour invasion into surrounding stroma and drug screening, *Biofabrication* 10 (2018) 034102, <https://doi.org/10.1088/1758-5090/aac70c>
- [45] A. Albanese, A.K. Lam, E.A. Sykes, J.V. Rocheleau, W.C. Chan, Tumour-on-a-chip provides an optical window into nanoparticle tissue transport, *Nat. Commun.* 4 (2013) 2718, <https://doi.org/10.1038/ncomms3718>
- [45] D. Bovard, A. Iskandar, K. Luettich, J. Hoeng, M.C. Peitsch, Organs-on-a-chip: A new paradigm for toxicological assessment and preclinical drug development, *Toxicology Research and Application* 1 (2017) 2397847317726351, <https://doi.org/10.1177/2397847317726351>
- [47] H.F. Wang, Y. Liu, T. Wang, G. Yang, B. Zeng, C.X. Zhao, Tumor-Microenvironment-on-a-Chip for Evaluating Nanoparticle-Loaded Macrophages for Drug Delivery, *ACS Biomater. Sci. Eng.* 6 (2020) 5040-5050, <https://doi.org/10.1021/acsbiomaterials.0c00650>
- [48] H.-F. Wang, R. Ran, Y. Liu, Y. Hui, B. Zeng, D. Chen, D.A. Weitz, C.-X. Zhao, Tumor-Vasculature-on-a-Chip for Investigating Nanoparticle Extravasation and Tumor Accumulation, *ACS Nano* 12 (2018) 11600-11609, <https://doi.org/10.1021/acsnano.8b06846>
- [49] Q. Sun, S.H. Tan, Q. Chen, R. Ran, Y. Hui, D. Chen, C.-X. Zhao, Microfluidic Formation of Coculture Tumor Spheroids with Stromal Cells As a Novel 3D Tumor Model for Drug Testing, *ACS Biomater. Sci. Eng.* 4 (2018) 4425-4433, <https://doi.org/10.1021/acsbiomaterials.8b00904>
- [50] J. Friend, L. Yeo, Fabrication of microfluidic devices using polydimethylsiloxane, *Biomicrofluidics* 4 (2010), Artn 026502, <https://doi.org/10.1063/1.3259624>
- [51] V. Velasco, S.A. Shariati, R. Esfandyarpour, Microtechnology-based methods for organoid models, *Microsyst. Nanoeng.* 6 (2020) 76, <https://doi.org/10.1038/s41378-020-00185-3>
- [52] X. Liu, J. Fang, S. Huang, X. Wu, X. Xie, J. Wang, F. Liu, M. Zhang, Z. Peng, N. Hu, Tumor-on-a-chip: from bioinspired design to biomedical application, *Microsyst. Nanoeng.* 7 (2021) 50, <https://doi.org/10.1038/s41378-021-00277-8>

- [53] M. Kitsara, D. Kontziampasis, O. Agbulut, Y. Chen, Heart on a chip: Micro-nanofabrication and microfluidics steering the future of cardiac tissue engineering, *Microelectron. Eng.* 203-204 (2019) 44-62, <https://doi.org/10.1016/j.mee.2018.11.001>
- [54] Z. Huang, G. Chi-Pong Tsui, Y. Deng, C.-Y. Tang, Two-photon polymerization nanolithography technology for fabrication of stimulus-responsive micro/nano-structures for biomedical applications, *Nanotechnol. Rev.* 9 (2020) 1118-1136, <https://doi.org/10.1515/ntrev-2020-0073>
- [55] A.-I. Bunea, N. del Castillo Iniesta, A. Droumpali, A.E. Wetzel, E. Engay, R. Taboryski, Micro 3D Printing by Two-Photon Polymerization: Configurations and Parameters for the Nanoscribe System, *Micro* 1 (2021), <https://doi.org/10.3390/micro1020013>
- [56] G. Kumi, C.O. Yanez, K.D. Belfield, J.T. Fourkas, High-speed multiphoton absorption polymerization: fabrication of microfluidic channels with arbitrary cross-sections and high aspect ratios, *Lab Chip* 10 (2010) 1057-1060, <https://doi.org/10.1039/B923377F>
- [57] M. Tse Janet, G. Cheng, A. Tyrrell James, A. Wilcox-Adelman Sarah, Y. Boucher, K. Jain Rakesh, L. Munn Lance, Mechanical compression drives cancer cells toward invasive phenotype, *Proc. Natl. Acad. Sci. U S A* 109 (2012) 911-916, <https://doi.org/10.1073/pnas.1118910109>
- [58] F. Broders-Bondon, T.H. Nguyen Ho-Bouidoires, M.-E. Fernandez-Sanchez, E. Farge, Mechanotransduction in tumor progression: The dark side of the force, *J Cell Biol* 217 (2018) 1571-1587, <https://doi.org/10.1083/jcb.201701039>
- [59] Q. Liu, Q. Luo, Y. Ju, G. Song, Role of the mechanical microenvironment in cancer development and progression, *Cancer Biol Med* 17 (2020) 282-292, <https://doi.org/10.20892/j.issn.2095-3941.2019.0437>
- [60] S.P. Desai, D.M. Freeman, J. Voldman, Plastic masters—rigid templates for soft lithography, *Lab Chip* 9 (2009) 1631-1637, <https://doi.org/10.1039/B822081F>
- [61] G. Lazzari, V. Nicolas, M. Matsusaki, M. Akashi, P. Couvreur, S. Mura, Multicellular spheroid based on a triple co-culture: A novel 3D model to mimic pancreatic tumor complexity, *Acta Biomater.* 78 (2018) 296-307, <https://doi.org/10.1016/j.actbio.2018.08.008>
- [62] N. Bidan, S. Lores, A. Vanhecke, V. Nicolas, S. Domenichini, R. López, M. de la Fuente, S. Mura, Before *in vivo* studies: *In vitro* screening of sphingomyelin nanosystems using a relevant 3D multicellular pancreatic tumor spheroid model, *Int. J. Pharm.* (2022) 121577, <https://doi.org/10.1016/j.ijpharm.2022.121577>

[63] J. Lachaux, G. Hwang, N. Arouche, S. Naserian, A. Harouri, V. Lotito, C. Casari, T. Lok, J.B. Menager, J. Issard, J. Guihaire, C.V. Denis, P.J. Lenting, A.I. Barakat, G. Uzan, O. Mercier, A.-M. Haghiri-Gosnet, A compact integrated microfluidic oxygenator with high gas exchange efficiency and compatibility for long-lasting endothelialization, *Lab Chip* 21 (2021) 4791-4804, <https://doi.org/10.1039/D1LC00356A>